Fibroblast Adaptation and Stiffness Matching to Soft Elastic Substrates

Jérôme Solon,*† Ilya Levental,*‡ Kheya Sengupta,*¶ Penelope C. Georges,*‡ and Paul A. Janmey*§
*Institute for Medicine and Engineering, University of Pennsylvania, Philadelphia, Pennsylvania 19104; †European Molecular Biology Laboratory, 69117, Heidelberg, Germany; ‡Department of Bioengineering, and §Departments of Physiology and Physics, University of Pennsylvania, Philadelphia, Pennsylvania 19104; and ¶CRMC-N UPR CNRS 7251, Luminy, Marseille, France

ABSTRACT Many cell types alter their morphology and gene expression profile when grown on chemically equivalent surfaces with different rigidities. One expectation of this change in morphology and composition is that the cell's internal stiffness, governed by cytoskeletal assembly and production of internal stresses, will change as a function of substrate stiffness. Atomic force microscopy was used to measure the stiffness of fibroblasts grown on fibronectin-coated polyacrylamide gels of shear moduli varying between 500 and 40,000 Pa. Indentation measurements show that the cells' elastic moduli were equal to, or slightly lower than, those of their substrates for a range of soft gels and reached a saturating value at a substrate rigidity of 20 kPa. The amount of cross-linked F-actin sedimenting at low centrifugal force also increased with substrate stiffness. Together with enhanced actin polymerization and cross-linking, active contraction of the cytoskeleton can also modulate stiffness by exploiting the nonlinear elasticity of semiflexible biopolymer networks. These results suggest that within a range of stiffness spanning that of soft tissues, fibroblasts tune their internal stiffness to match that of their substrate, and modulation of cellular stiffness by the rigidity of the environment may be a mechanism used to direct cell migration and wound repair.

INTRODUCTION

Most cells in multicellular organisms are embedded in tissues composed of other cells or extracellular matrices with well-defined elastic moduli that span a range from ~100 Pa for very soft tissues such as fat or brain to >10,000 Pa for muscle, and even greater stiffnesses for cartilage and bone (1). In contrast, cells grown on glass or plastic surfaces, or in many synthetic matrices, generally attach and pull on materials with elastic moduli on the order of gigapascals. Recent experiments have shown that the mechanical properties of a cell's microenvironment can have as great an impact on cell structure and function as soluble stimuli and cell-cell contacts (2–4). Cells grown on stiff substrates assemble actin stress fibers (5), exhibit a more spread phenotype (3), upregulate the expression of integrins (6), modify the properties and composition of their substrate adhesions (3,7,8), and activate signaling pathways characteristic of contractility (7,9,10). Stimulated contractility leads to an increase in the stress applied to cellular substrates (7,11), which has been shown to regulate the activity of small GTPases and the formation of focal adhesions (10,12). These responses are cell-type dependent in that the effective range of substrate rigidity depends on the tissue type from which the cells are derived (4). For example, fibroblasts achieve maximal spreading at substrate stiffness of ~10 kPa (6), whereas neurons branch more avidly on softer surfaces (<0.5 kPa) (13), and chondrocytes only begin to spread at 10 kPa (14). Similarly, differentiation of myoblasts into myotubes occurs only on substrate compliances mimicking those of differentiated muscle (~10 kPa) (15). Motility of cultured myocytes also depends on substrate stiffness, with a maximal rate of motility found at intermediate stiffness between 21 kPa and 52 kPa depending on the density of adhesive ligand (16). Matrix stiffness also affects cell proliferation (17) and differentiation. For example, mesenchymal stem cells can be differentiated into neurogenic, myogenic, or osteogenic cell types by varying the magnitude of matrix stiffness to mimic that of the native tissue (2).

Not all cell types appear to be sensitive to substrate stiffness, and not all mechanosensitive cell types respond similarly to changes in stiffness. However, of the cell types studied thus far, most spread more and adhere better to harder matrices, and some cannot grow at all on very soft (<50 Pa) surfaces (3,5,15,17–19). A current hypothesis to explain increased spreading on stiffer adhesive surfaces is that by pulling on the matrix at focal adhesions, the cell creates tension within its membrane and in the underlying cortical actin mesh (20). The magnitude of the tension depends on the material properties of the matrix: a relatively stiff matrix will resist cellular force more than a soft one. In cell types that grow preferentially on hard matrices, the tension will stimulate such a cell to extend about its periphery (21). Micromechanical stimulation experiments with optical tweezers and magnetic bead cytometry have shown that integrin-mediated linkage between the cytoskeleton and extracellular matrix is reinforced on application of force (9,22,23). Focal adhesions, the loci of interaction between the cytoskeleton and adhesion proteins, are highly dynamic and mechanosensitive, changing their size, shape, and number in response to substrate stiffness and applied stress

Submitted November 20, 2006, and accepted for publication June 21, 2007.

Jérôme Solon and Ilya Levental contributed equally to this work.

Address reprint requests to Dr. Paul Janmey, 1010 Vagelos Labs, 3340 Smith Walk, Philadelphia, PA 19104. Tel.: 215-573-7380; Fax: 215-573-6815; E-mail: janmey@mail.med.upenn.edu.

Editor: Elliot L. Elson.

0006-3495/07/12/4453/09 $2.00

doi: 10.1529/biophysj.106.101386

(7,8,12,24), and these changes in turn can alter the assembly state of the cytoskeleton and the tension imposed on it by activated myosins or other motors. Because of the nonlinear elasticity of many biopolymer networks, imposition of internal tension can lead to changes in stiffness even in the absence of changes in assembly (25,26).

In this article, we report the influence of substrate stiffness on the mechanical properties of fibroblasts, specifically on cell size, cytoskeleton organization, and cell stiffness. To probe cell stiffness, we employed atomic force microscopy (AFM), both as an imaging modality and as a microindenter/force transducer. By varying substrate stiffness using a well-established polyacrylamide (PA) gel method (27) and measuring cell stiffness, we have observed that cells not only change their size and cytoskeletal organization but also adapt their stiffness to match the compliance of their substrate.

MATERIAL AND METHODS

Bis-acrylamide-PA gel fabrication

Mixed acrylamide (7.5%) and bis-acrylamide (0.03–3%) solutions (Fisher, Hampton, NH) were polymerized using ammonium persulfate and *N*,*N*,*N*′,*N*′-tetramethylethylenediamine, as described previously (6), following a method developed by Pelham and Wang (3,27). A toluene solution saturated with *N*-succinimidyl acrylate was layered between the unpolymerized aqueous acrylamide solution and the top coverslip to allow covalent modification of the gel with an extracellular matrix ligand. After polymerization of the cross-linked acrylamide solution, the surface of the gel was reacted with a 0.2 mg/ml solution of human fibronectin (Invitrogen, Carlsbad, CA) in phosphate-buffered saline (PBS). The gels were then taped to petri dishes, sterilized under ultraviolet light for 30 min, and incubated with fibroblast culture medium for 1 h before plating of the cells. AFM experiments were performed 24 h after plating to ensure complete spreading of the cells. Protein concentration at the surface of the gel is independent of gel stiffness or bis-acrylamide concentration with this method (28).

Cell culture and immunostaining

NIH-3T3 fibroblasts were cultured with DMEM (BioWhittaker, Walkersville, MD) supplemented with 10% fetal bovine serum (Hyclone, Logan, UT) at 37°C with 5% CO_2. At 24 h after plating, cells were fixed with 4% paraformaldehyde (Sigma-Aldrich) at 37°C for 30 min, and the fixation reaction was quenched with 50 mM ammonium chloride (Sigma-Aldrich) for 5 min. The samples were blocked and permeabilized with 1% bovine serum albumin (Sigma-Aldrich) and 0.2% Triton (Sigma-Aldrich) for 30 min. F-actin was then specifically labeled with 1:40 rhodamine-phalloidin (Invitrogen) in PBS for 30 min.

Western blot analysis and densitometry

After 24 h of plating on PA gels, cells were washed with ice-cold PBS, followed by inversion of the coverslips (gel side down) into 250 μL of RIPA buffer (Millipore, Billerica, MA) in a plastic dish for 5 min. The gels were then rubbed against the plastic dish by scraping the top of the coverslip for another 5 min, followed by gentle scraping of the gel surface. The cell lysate was centrifuged for 10 min at 13,000 rpm and 4°C, supernatant was discarded, and the pellet was washed with ice-cold PBS and centrifuged again. This pellet contains insoluble intracellular proteins, including all of the cross-linked actin filaments in the cell. The pellet was subjected to SDS-PAGE and imaged using the ECL system according to the manufacturer's instructions (primary—mouse anti-β-actin, Sigma-Aldrich; secondary—sheep antimouse, Sigma-Aldrich). Densitometry was performed using MultiGauge V3.0 from FujiFilm (Tokyo, Japan).

Atomic force microscopy and epifluorescence microscopy

The AFM used was a Bioscope (DAFM-2X, Veeco, Woodbury, NY) mounted on an epifluorescence microscope (Axiovert 100, Zeiss, Thornwood, NY). The AFM was used to estimate the stiffness (elastic modulus) of the cell and of the gel on which the cell adheres. Indentation was done with a silicon nitride cantilever with a conical tip. The cantilever used for these experiments was 196 μm long, 23 μm wide, and 600 nm thick, with a spring constant of 0.06 N/m (DNP, Veeco). The gel and the cells were ''force volume'' imaged, i.e., we obtained a height and stiffness map of both a cell and the surrounding gel. The measured area was a 30 μm $\times$ 30 μm map with at least 32 points per direction (see Fig. 2, *E* and *F*). Cell stiffness was quantified by indenting each measured cell at three distinct spots, with the average from those three measurements defined as the cell stiffness. Additionally, the gel immediately adjacent to the cell was probed. Repeated probing of the same point on a cell yielded identical stiffness measurements, whereas the spot-to-spot variation in stiffness was 10–20%.

To quantify the stiffness, the first 400 nm of tip deflection from the horizontal (Δd) were fit with the Hertz model modified for a cone (29)

$$\Delta d = \frac{k}{4A} + \Delta z + \frac{1}{2}\sqrt{\left(\frac{k}{A}\right)^2 + 4\frac{k\Delta z}{A}} \quad \text{and}$$

$$A = \frac{2}{\pi}\tan(\alpha)\frac{E}{1-\nu^2},$$

where k and Δz are the bending rigidity and the vertical indentation of the cantilever, E is the Young's modulus, α is the cone tip angle, and ν the Poisson ratio. Young's modulus is the ratio between the strain ($\delta z/z$) applied to the material and the resulting stress. The Poisson ratio is defined as the ratio of compression strain in the direction normal to the applied stress and the extensional strain in the direction of the applied stress and is taken to be 0.5 for all samples. The outermost protrusions of the cell were usually 100–200 nm thick, whereas the rest of the imaged area was up to 1.5 μm in height.

There are significant limitations to using the Hertz model for indentations of very thin elastic materials adhered to rigid surfaces, requiring more complex analyses (30). For the measurements presented here, using only the initial 400 nm of tip deflection as well as measuring only those parts of the cells that were >700 nm (see Results) in height, avoided these complications, as confirmed by the agreement between elastic moduli of gels measured by AFM and macroscopic rheologic methods. Moreover, regardless of the multiple factors that prevent assigning a precise numerical value of elastic modulus for a complex, heterogeneous viscoelastic body such as a cell, relative differences in stiffness between conditions can still be measured.

RESULTS

Characterization of the mechanical properties of PA gels

Fibronectin-laminated PA gels present a smooth surface with homogeneous stiffness as measured by AFM using force-volume imaging to obtain a high-resolution topographic image as well as a pixel-by-pixel map of the stiffness of the gel. Fig. 1 *A* shows a typical deflection-indentation curve used to calculate elastic moduli derived from indentations of

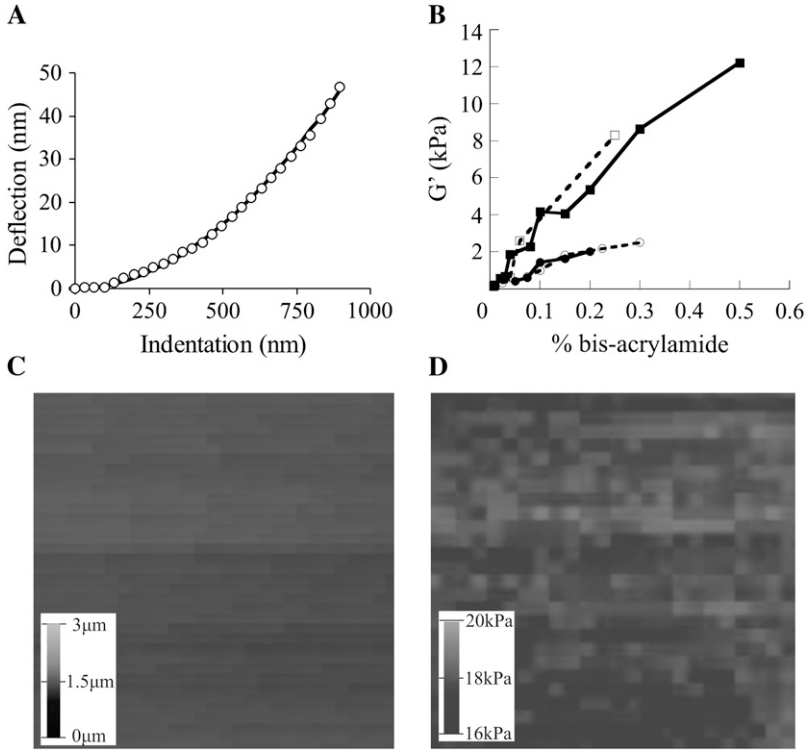

FIGURE 1 Polyacrylamide gel characterization by AFM. (*A*) Representative curve of cantilever deflection as a function of tip indentation into a 5-kPa PA gel (*circles*) and the fit to the data with the Hertz model (*bold line*). (*B*) PA gel stiffness as a function of bis-acrylamide cross-linker concentration (*open squares*/*dashed line*, AFM 7.5% acrylamide; *solid squares*/*solid line*, macroscopic rheology 7.5% acrylamide; *open circles*/*dashed line*, AFM 5% acrylamide (8); *solid circles*/*solid line*, macroscopic rheology 5% acrylamide). (*C*) Topographical map of the surface of a 5-kPa PA gel. Scale, 30 μm × 30 μm. (*D*) Stiffness map of the surface of a 5-kPa PA gel. Scale, 30 μm × 30 μm.

<1500 nm into the surface of gels with an average thickness of 50 μm. The small ratio of indentation depth to sample thickness suggests that the simplifying assumptions used to calculate elastic moduli are appropriate, and the good fit of data to the Hertz formula confirms that these gels are well approximated as semiinfinite elastic media.

The validity of using the Hertz model to infer Young's moduli from force-indentation curves was further tested by comparing stiffness values obtained from AFM indentation of the gels as a function of cross-linker concentration to values of shear modulus determined by bulk rheology measurements using methods described previously (6) (Fig. 1 *B*). The close agreement between the two data sets confirms that the cross-linked PA gels behave as linear elastic materials and that AFM indentation provides accurate measurements of the local elastic moduli of micrometer-scale-thickness solids with moduli in the range of 200–10,000 Pa. Fig. 1 *C* shows a height map of a 15-kPa gel measured by the AFM in imaging mode. The variation in height is <10% over the 30-μm scale on which cells are typically imaged. The stiffness of the same gel was measured using the force mode of the AFM. The stiffness map in Fig. 1 *D* shows similar uniformity to the height map with no sharp features that would present substantially softer or stiffer regions to the cell.

Visualization of actin cytoskeleton structure

The actin cytoskeletons of fibroblasts adhering to gels of varying elastic moduli were visualized by staining F-actin with phalloidin after fixation. In cells adherent to gels of stiffness between 1 and 5 kPa, the actin structure is not organized into stress fibers but instead shows diffuse cortical actin distributed relatively evenly over the cell volume (see Fig. 3 *A1* and *A2*). In contrast, on a 10-kPa gel, fibroblasts begin to exhibit the more organized, bundled actin structures typical of stress fibers (see Fig. 3 *A3*). Finally, on glass ($E \sim$ 1 GPa), the actin cytoskeleton is largely organized into stress fibers that are both larger and more developed than those on 10-kPa gels. These data show that compliance of the substrate significantly affects the organization of the actin cytoskeleton and likely the mechanical properties of the cell.

Measurement of the mechanical properties of fibroblasts

Using AFM, we force-volume imaged both cells and the substrate around the cell on substrates of varying compliances 24 h after plating. Fig. 2 *A* shows a representative trace of cantilever deflection as a function of tip indentation and retraction into the cell as well as the Hertz model fit to the data (*solid line*, indentation; *dashed line*, retraction). Hysteresis on retraction of the cantilever at the rates used was small enough to be impractical to quantify, confirming the mainly elastic behavior of the cells under these conditions of small strains on a subsecond time scale (Fig. 2 *A*). Fig. 2 *D* is a compilation of many extension-retraction curves comprising a stiffness map of a fibroblast adhering to a fibronectin-coated glass substrate. The cell stiffness is heterogeneous

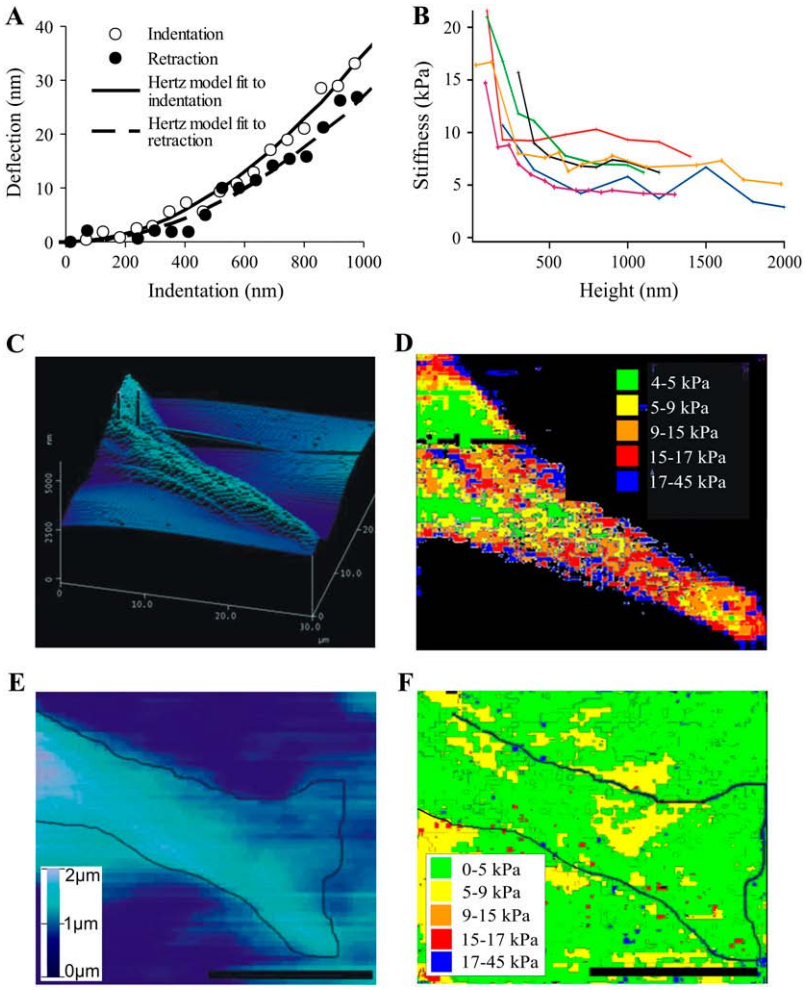

FIGURE 2 Fibroblast characterization by AFM. (*A*) Representative curve of cantilever deflection as a function of tip indentation into (*open circles*) and retraction from (*solid circles*) a fibroblast plated on a fibronectin-laminated 5-kPa PA gel and the fit to the data with the Hertz model (*solid line*, indentation; *dashed line*, retraction). (*B*) Variation in measured cell stiffness as a function of cell height from the substrate (fibronectin-coated glass) for several individual cells. Each curve represents a single cell. (*C*) Topographical map of the edge of a fibroblast adhering to a glass substrate. Scale, 30 μm $\times$ 30 μm. (*D*) Stiffness map of the edge of a fibroblast adhering to a glass substrate coated with fibronectin. Scale, 30 μm $\times$ 30 μm. (*E*) Topographical map of the edge of a fibroblast adhering to a fibronectin-laminated 5-kPa PA gel. Bold line shows the outline of the cell. Scale bar = 10 μm. (*F*) Stiffness map of the edge of a fibroblast adhering to a fibronectin-laminated 5-kPa PA gel. Scale bar = 10 μm.

from 5 kPa in the parts of the cell proximal to the cell body to 17 kPa in the most distal regions. The stiffest part of the cell corresponds to the edge of the cell, which also corresponds to the lowest part of the cell (see Fig. 2 *C*). The higher parts of the cell are more homogeneous and softer (Fig. 2, *C* and *D*). This variation in cell stiffness is likely caused by contributions from both the stiffness of the substrate (glass in Fig. 2, *C* and *D*) at low cell height and also by the higher density and cross-link content of the actin at the edge of the cell. The possible contribution of substrate stiffness presents a critical problem for accurate quantitative determination of the cell's elastic modulus. To account for this problem, we studied the effect of a stiff substrate on apparent cell stiffness as a function of the height at which the measurement was taken. Correlating the height of the cell from the substrate to the measured stiffness of the cell (Fig. 2 *B*), we observed a high degree of correlation for cell heights $<$700 nm, whereas above 700 nm, the measured modulus remained constant as a function of height. This finding suggests that the strain caused by the deformation, δ, of the tip indenting the cell is distributed within the cell body and is not transmitted to the stiff substrate below when the cell is thicker than $\sim$700 nm.

Effect of gel compliance on fibroblast area and stiffness

In contrast to cells on glass, fibroblasts plated on soft PA gels are more uniform in both stiffness and height (Fig. 2, *E* and *F*). To measure the effect of substrate stiffness on fibroblast elastic moduli without complications from the inadequacy of the Hertz model for very thin samples and large indentations, we estimated the modulus by fitting force-indentation data only for indentations $<$400 nm, and only for cell heights between 1 μm and 2 μm above the substrate, where stiffness is uncorrelated with height and substrate stiffness. For each fibroblast, we measured the area and the stiffness of the cell as well as the stiffness of the PA substrate around the cell, which allowed us to account for local lateral variations in gel stiffness. Fig. 3 *B* shows the variation of the cell area as a function of the stiffness of the gel on which the cell adheres. Fibroblasts spread three times more on 10-kPa gels, where the cell area is $\sim$1500 μm^2, than on 2-kPa gels, where the cell area is only 500 μm^2, despite the lack of well-organized stress fibers in cells plated on this range of soft PA gels (Fig. 3 *A*). On stiffer gels, and even on glass, the cell area does not significantly increase from the area on 10-kPa gels (Fig. 3 *B*).

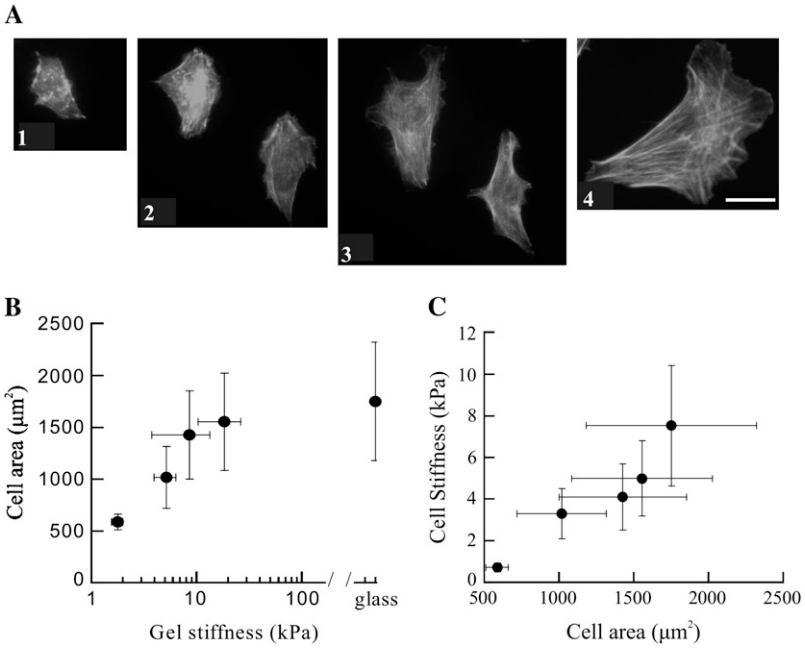

FIGURE 3 Microscopic analysis of fibroblasts on gels. (*A*) Rhodamine-phalloidin staining of the F-actin of fixed fibroblasts on a 1-kPa gel (*1*), 5-kPa gel (*2*), 10-kPa gel (*3*), and glass (*4*). Bar, 40 μm. (*B*) Projected cell area as a function of gel stiffness. Each point on the graph is a mean ± SD of 12–40 different cells. (*C*) Cell stiffness as a function of cell area. Each point on the graph is a mean ± SD of 12–40 different cells.

The stiffness of fibroblasts is also strongly correlated with the cell area (Fig. 3 *C*). The average stiffness of the fibroblasts increased from 1 to 8 kPa as the cell area increased from 600 to 1800 μm^2. A slight increase in stiffness from 6 to 8 kPa was also observed between cells on 20-kPa gels and cells on glass, correlated with the more organized thicker stress fibers observed on glass (Fig. 3 *A4*). Measuring the substrate next to each cell allows correlation of cell stiffness with local gel stiffness for each cell measured. The raw data shown in Fig. 4 *B*, where each point represents the stiffness of a single cell and that of the immediately adjacent gel, reveal that the stiffness of the fibroblasts follows closely the stiffness of the substrate (*dark line* in Fig. 4 *B* and *inset* of Fig. 4 *B*) between 800 Pa and 4 kPa, while almost always remaining slightly softer. This finding suggests that in the range of stiffness of soft tissues in which native fibroblasts reside, there is a quantitative adaptability of the cell to its mechanical environment. Only at very high substrate stiffness (>10 kPa) do these cells fail to match substrate stiffness, and at this point stress fibers appear.

DISCUSSION

Previous studies have shown that altering the stiffness of the underlying substrate under conditions that maintain a constant chemical environment can lead to very large changes in the rates at which cells move or divide, the force with which they pull on the substrate, whether or not they form actin stress fibers or sarcomeres, and whether or not they survive (reviewed by Discher et al. (4)). Changes in cytoskeletal tension caused by alterations in substrate stiffness can lead to changes in specific protein levels by both proteolytic and transcriptional regulation (27). Previous quantitative studies of the graded response of adherent cells to substrate stiffness have focused on measures of cell shape, motility, and development of traction forces or on the stiffness-dependent expression of specific gene products. The changes in cytoskeletal structure have suggested that the cells' internal stiffness may also depend on substrate stiffness.

By employing concurrent measurement of actin cytoskeleton structure, cell height, area, and stiffness, we quantified the morphological and physical properties of fibroblasts as a function of the compliance of their substrate. Here, we have used an AFM cantilever as a microindenter to determine the mechanical properties of the cells. Because the magnitude of indentation into the cell is relatively small (<400 nm) compared with the height of the cell where it is probed, the elastic resistance to indentation reflects the stiffness of the cortical actin network. For a range of substrate stiffness from 1 to 5 kPa, fibroblasts adjust their average stiffness, without formation of stress fibers, to match that of the substrate on which they adhere. As the substrate stiffness increases past this 5-kPa range, the cells remain softer than their substrate, presumably because they reach the limit of the mechanism by which they reinforce their cytoskeletons. Stress fibers become prevalent only on these stiffer substrates. These findings define two different states of cell adhesion and spreading: on soft substrates the cell is not fully spread and has a cortical actin cytoskeleton but no stress fibers, whereas on a stiff substrate the cell becomes more completely spread and organizes the actin cytoskeleton into stress fibers. The change in actin organization is confirmed by the increased amount of actin sedimenting at low centrifugal force (Fig. 5) from extracts of cells grown on very stiff substrates.

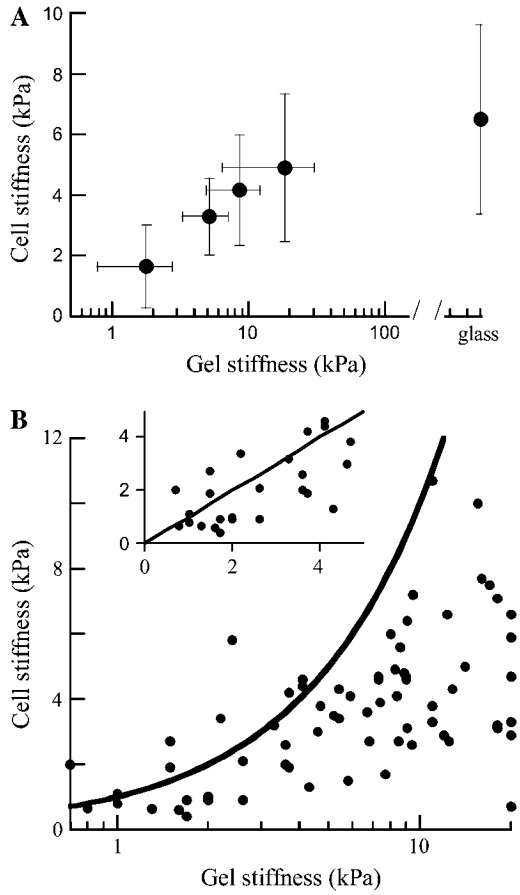

FIGURE 4 Effect of substrate stiffness on cell stiffness. (*A*) Cell stiffness as a function of the stiffness of the adjacent gel. Each point is a mean ± SD of 12–40 different cells. (*B*) Individual measurements of cell stiffness as a function of adjacent gel stiffness. Each point shown is the mean stiffness of a single cell plotted against that of the neighboring gel. Bold line is the line of identity showing the gel stiffness. The inset is an enlargement of the range of gel stiffness up to 5 kPa on a linear scale.

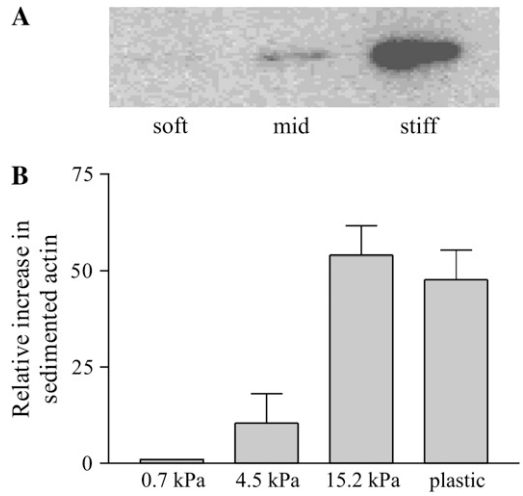

FIGURE 5 Effect of substrate stiffness of F-actin organization. (*A*) Western blot for actin from pellet formed by low-speed (15,000 × *g*) centrifugation of fibroblast lysates. Cells were lysed 24 h after plating on fibronectin-laminated PA gels with 0.7 kPa, 4.5 kPa, and 15.2 kPa elastic moduli. (*B*) Densitometric quantification of Western blots for actin sedimenting at low speed from fibroblasts plated on PA gels of 0.7 kPa, 4.5 kPa, 15.2 kPa, or tissue culture plastic. All values normalized to total protein in cell lysate. Error bars are representative standard deviations from three repeats.

A limitation of the current measurements and their interpretation is that the mechanical measurements are made at a single frequency of 1 Hz, and the force-indentation curves are fit with a purely elastic model, neglecting viscous effects that are likely to be important for deformations at longer times or for larger strains (31). The quality of the fits to the data shown in Figs. 1 *A* and 2 *A* supports the conclusion that at this frequency and degree of deformation the cell periphery is nearly as elastic as a PA gel. However, it is known that the cytoskeleton is viscoelastic, and many recent studies have emphasized the frequency or time dependence of cell rheology (32). Despite this inherent viscoelasticity, the soft glassy model of cell rheology in which the cell has no permanent elasticity predicts that the time dependence of cytoskeletal stiffness is very weak, and much of the deformation on a time scale of seconds is elastically recoverable. If it were possible to make measurements on a time scale of hours, the elastic modulus of the PA substrate would not change from its value at 1 Hz, whereas the apparent modulus of the cell would be near zero. Such a measurement is not practically achievable because at long times deformation of a cell will be caused by both viscous flow and active remodeling, and these two processes cannot currently be distinguished rheologically. The potential importance of the rate of deformation raises the question of the relevant time over which the cell probes its environment to respond by changing its internal stiffness. The finding that cell elastic moduli measured on a 1-Hz time scale match those of their substrate suggests that the signals regulating cytoskeletal adaptation, which presumably originate at adhesion sites, are repeatedly probed on a time scale on the order of seconds as the cells spread and attach.

The response of the fibroblast to increased substrate stiffness in the range from 500 Pa to 10 kPa involves a reorganization of the cytoskeleton to produce a more organized system of filament bundles and increasing amounts of cross-linked actin filaments as seen in Fig. 5 and in previous reports (5,6,8,33). Other studies of fibroblasts or other cell types have shown α-smooth muscle actin expression (34), production of calponin (35), expression of filamin (36), and reorganization and change in the of type of intermediate filament expressed (37,38) to be important in regulating the mechanical response of adherent cells. One outcome of these changes in cytoskeletal proteins is likely to be reinforcement of the intracellular protein networks and their attachment to the membrane. Other mechanisms that do not involve changes in protein levels or biochemical interactions can also stiffen the cell.

Production of internal tension, sometimes called prestress, has previously been proposed as a mechanism to change a cell's mechanical properties (39–41). Tension-induced stiffening is an outcome of some tensegrity models with specific geometries (42), but it is also a consequence of the nonlinear elasticity of semiflexible networks even in isotropic arrangements (26,43). This effect has been demonstrated in vitro by myosin-induced tension stiffening of isotropic actin networks (44). The variation of cell size, stiffness, and traction force on soft substrates is consistent with a simple model of a nonlinear, variable stiffness gel (the cell) spreading on and adhering to a linear gel of constant stiffness (the PA substrate). Based on recent studies of the strain stiffening of whole cells (45), the cell is modeled as a nonlinear elastic gel of elastic modulus $E_c(\varepsilon_c)$, where $E_c(\varepsilon_c)$ is a function that increases with strain, ε_c. Here, stress is applied to the system by the cell adhering and spreading as a result of adhesion energy between the cell and the substrate of constant modulus E_g. As the cell spreads and is deformed, $E_c(\varepsilon_c)$ increases with spreading, i.e., with the deformation of the cell, ε_c. The stress σ generated by the spreading of the cell is proportional to the deformation of both the cell and the gel by the elastic moduli,

$$\sigma = E_c(\varepsilon_c) * \varepsilon_c \quad \text{and} \quad \sigma = E_g * \varepsilon_g,$$

respectively, where E_g is the (constant) elastic modulus of the gel and ε_g is the strain of the gel. A force balance yields an expression for the deformation of the cell ε_c as a function of the deformation of the gel ε_g and the elastic modulus of the cell $E_c(\varepsilon_c)$,

$$\varepsilon_c = \frac{E_g}{E_c(\varepsilon_c)}\varepsilon_g.$$

This explanation is comparable to the model of a cell and its substrate as a two-spring system where the elasticity of the system is sensitive to the softer spring (46). As long as the stiffness of the cell $E_c(\varepsilon_c)$ is lower than the stiffness of the gel E_g, strain applied to the system by adhesion will result in a cell deformation that will be greater than the deformation of the gel. For an incremental deformation of a soft cell, the stiffer gel will not deform. As the soft cell continues to spread and deform, the stiffness of the cell will increase with ε_c. When the cell deforms to the point that its stiffness is the same as the stiffness of the gel ($E_c(\varepsilon_c) = E_g$), the substrate deformation will be equivalent to cell deformation. When this threshold is reached, further stress applied to the system leads to substrate deformation, and the cell deformation (spreading) will decrease and stop. If the gel is stiff enough, the cell spreads completely and organizes its cytoskeleton and adhesions. When this occurs, the cell enters a second state of adhesion, characterized by fully formed focal adhesions and stress fibers, and the simple description above is no longer applicable.

This highly simplified conceptual model of a spreading fibroblast as a nonlinear gel is consistent with numerous experiments. It qualitatively explains that there is a limit to cell stiffening caused by the stiffness of the gel on which it adheres, as observed in Fig. 4. It is also consistent with the fact that the size of the cells increases with increasing gel stiffness, as confirmed in Fig. 3 *A*, and in numerous other studies (3,6–8,28). The model also predicts that the stress between a fully spread cell and the gel will increase with gel stiffness, as was recently shown by traction force experiments (7,47). Experiments on fully spread MDCK cells also showed that the force applied by the cell on the substrate increased linearly with the stiffness of the substrate to produce an approximately constant substrate deformation (48). This result is qualitatively consistent with the model prediction that substrate deformation is the switch that controls cell spreading and stiffening, although quantification of this phenomenon would require knowledge of local cell and gel deformations that are not currently experimentally accessible. Additionally, if stiffer substrates allow more cell deformation than softer ones, as our model predicts, cells will tend to spread and migrate into stiffer regions, a phenomenon known as durotaxis that has been observed experimentally (19). According to these observations, persistent cell migration would require a substrate stiffer than the cell, and this form of durotaxis could be significant for understanding the impact of mechanical changes that occur in the basal lamina in pathological states.

The data presented here argue that the stiffness of the substrate is a critical regulator of cell morphology and behavior and that fibroblasts, and perhaps other cell types, increase their internal stiffness until they match that of their substrate. This observation implies that a cell does not have a predefined stiffness. The data of Fig. 4 show that individual fibroblast stiffness can vary by a factor of at least 25, and even population averages can vary by a factor of five as the substrate stiffness is altered. These variations are almost certainly underestimates because our current studies are limited to substrates stiffer than 1000 Pa, and other studies show that cells can sense differences between substrates softer than 100 Pa (13,28,49). The sensors that allow a cell to probe substrate stiffness are largely unknown, and not all cell types exhibit the same response to substrate compliance as shown here for fibroblasts. The sensitivity and cell-type specificity of responses to substrate stiffness suggest that mechanical probing of a cell's microenvironment may be an important element in formation, repair, and remodeling of tissues.

REFERENCES

1. Levental, I., P. C. Georges, and P. A. Janmey. 2007. Soft biological materials and their impact on cell function. *Soft Matter*. 1:299–306.
2. Engler, A. J., S. Sen, H. L. Sweeney, and D. E. Discher. 2006. Matrix elasticity directs stem cell lineage specification. *Cell*. 126:677–689.

3. Pelham, R. J., Jr., and Y. Wang. 1997. Cell locomotion and focal adhesions are regulated by substrate flexibility. *Proc. Natl. Acad. Sci. USA.* 94:13661–13665.
4. Discher, D. E., P. Janmey, and Y. L. Wang. 2005. Tissue cells feel and respond to the stiffness of their substrate. *Science.* 310:1139–1143.
5. Georges, P. C., and P. A. Janmey. 2005. Cell type-specific response to growth on soft materials. *J. Appl. Physiol.* 98:1547–1553.
6. Yeung, T., P. C. Georges, L. A. Flanagan, B. Marg, M. Ortiz, M. Funaki, N. Zahir, W. Ming, V. Weaver, and P. A. Janmey. 2005. Effects of substrate stiffness on cell morphology, cytoskeletal structure, and adhesion. *Cell Motil. Cytoskeleton.* 60:24–34.
7. Paszek, M. J., N. Zahir, K. R. Johnson, J. N. Lakins, G. I. Rozenberg, A. Gefen, C. A. Reinhart-King, S. S. Margulies, M. Dembo, D. Boettiger, D. A. Hammer, and V. M. Weaver. 2005. Tensional homeostasis and the malignant phenotype. *Cancer Cell.* 8:241–254.
8. Engler, A., L. Bacakova, C. Newman, A. Hategan, M. Griffin, and D. Discher. 2004. Substrate compliance versus ligand density in cell on gel responses. *Biophys. J.* 86:617–628.
9. Pourati, J., A. Maniotis, D. Spiegel, J. L. Schaffer, J. P. Butler, J. J. Fredberg, D. E. Ingber, D. Stamenovic, and N. Wang. 1998. Is cytoskeletal tension a major determinant of cell deformability in adherent endothelial cells? *Am. J. Physiol. Cell Physiol.* 274:C1283–1289.
10. Chrzanowska-Wodnicka, M., and K. Burridge. 1996. Rho-stimulated contractility drives the formation of stress fibers and focal adhesions. *J. Cell Biol.* 133:1403–1415.
11. Dembo, M., and Y. L. Wang. 1999. Stresses at the cell-to-substrate interface during locomotion of fibroblasts. *Biophys. J.* 76:2307–2316.
12. Riveline, D., E. Zamir, N. Q. Balaban, U. S. Schwarz, T. Ishizaki, S. Narumiya, Z. Kam, B. Geiger, and A. D. Bershadsky. 2001. Focal contacts as mechanosensors: externally applied local mechanical force induces growth of focal contacts by an mDia1-dependent and ROCK-independent mechanism. *J. Cell Biol.* 153:1175–1186.
13. Flanagan, L. A., Y. E. Ju, B. Marg, M. Osterfield, and P. A. Janmey. 2002. Neurite branching on deformable substrates. *Neuroreport.* 13: 2411–2415.
14. Subramanian, A., and H. Y. Lin. 2005. Crosslinked chitosan: its physical properties and the effects of matrix stiffness on chondrocyte cell morphology and proliferation. *J. Biomed. Mater. Res. A.* 75:742–753.
15. Engler, A. J., M. A. Griffin, S. Sen, C. G. Bonnemann, H. L. Sweeney, and D. E. Discher. 2004. Myotubes differentiate optimally on substrates with tissue-like stiffness: pathological implications for soft or stiff microenvironments. *J. Cell Biol.* 166:877–887.
16. Peyton, S. R., and A. J. Putnam. 2005. Extracellular matrix rigidity governs smooth muscle cell motility in a biphasic fashion. *J. Cell. Physiol.* 204:198–209.
17. Wang, H. B., M. Dembo, and Y. L. Wang. 2000. Substrate flexibility regulates growth and apoptosis of normal but not transformed cells. *Am. J. Physiol. Cell Physiol.* 279:C1345–C1350.
18. Reinhart-King, C., M. Dembo, and D. A. Hammer. 2003. Endothelial cell traction forces on RGD-derivatized polyacrylamide substrata. *Langmuir.* 19:1573–1579.
19. Lo, C. M., H. B. Wang, M. Dembo, and Y. L. Wang. 2000. Cell movement is guided by the rigidity of the substrate. *Biophys. J.* 79: 144–152.
20. Beningo, K. A., and Y. L. Wang. 2002. Flexible substrata for the detection of cellular traction forces. *Trends Cell Biol.* 12:79–84.
21. Schwarz, U. S., and S. A. Safran. 2002. Elastic interactions of cells. *Phys. Rev. Lett.* 88:048102.
22. Glogauer, M., P. Arora, G. Yao, I. Sokholov, J. Ferrier, and C. A. McCulloch. 1997. Calcium ions and tyrosine phosphorylation interact coordinately with actin to regulate cytoprotective responses to stretching. *J. Cell Sci.* 110:11–21.
23. von Wichert, G., B. Haimovich, G. S. Feng, and M. P. Sheetz. 2003. Force-dependent integrin-cytoskeleton linkage formation requires down-regulation of focal complex dynamics by Shp2. *EMBO J.* 22:5023–5035.
24. Balaban, N. Q., U. S. Schwarz, D. Riveline, P. Goichberg, G. Tzur, I. Sabanay, D. Mahalu, S. Safran, A. Bershadsky, L. Addadi, and B. Geiger. 2001. Force and focal adhesion assembly: a close relationship studied using elastic micropatterned substrates. *Nat. Cell Biol.* 3: 466–472.
25. Shah, J. V., and P. A. Janmey. 1997. Strain hardening of fibrin gels and plasma clots. *Rheologica Acta.* 36:262–268.
26. Storm, C., J. J. Pastore, F. C. MacKintosh, T. C. Lubensky, and P. A. Janmey. 2005. Nonlinear elasticity in biological gels. *Nature.* 435:191–194.
27. Beningo, K. A., C. M. Lo, and Y. L. Wang. 2002. Flexible polyacrylamide substrata for the analysis of mechanical interactions at cell-substratum adhesions. *Methods Cell Biol.* 69:325–339.
28. Georges, P. C., W. J. Miller, D. F. Meaney, E. Sawyer, and P. A. Janmey. 2006. Matrices with compliance comparable to that of brain tissue select neuronal over glial growth in mixed cortical cultures. *Biophys. J.* 90:3012–3018.
29. Domke, J., and M. Radmacher. 1998. Measuring the elastic properties of thin polymer films with the atomic force microscope. *Langmuir.* 14:3320–3325.
30. Mahaffy, R. E., S. Park, E. Gerde, J. Kas, and C. K. Shih. 2004. Quantitative analysis of the viscoelastic properties of thin regions of fibroblasts using atomic force microscopy. *Biophys. J.* 86:1777–1793.
31. Bursac, P., G. Lenormand, B. Fabry, M. Oliver, D. A. Weitz, V. Viasnoff, J. P. Butler, and J. J. Fredberg. 2005. Cytoskeletal remodelling and slow dynamics in the living cell. *Nat. Mater.* 4:557–561.
32. Balland, M., N. Desprat, D. Icard, S. Fereol, A. Asnacios, J. Browaeys, S. Henon, and F. Gallet. 2006. Power laws in microrheology experiments on living cells: Comparative analysis and modeling. *Phys. Rev. E Stat. Nonlin. Soft Matter Phys.* 74:021911.
33. Tan, J. L., J. Tien, D. M. Pirone, D. S. Gray, K. Bhadriraju, and C. S. Chen. 2003. Cells lying on a bed of microneedles: an approach to isolate mechanical force. *Proc. Natl. Acad. Sci. USA.* 100:1484–1489.
34. Hinz, B., G. Celetta, J. J. Tomasek, G. Gabbiani, and C. Chaponnier. 2001. Alpha-smooth muscle actin expression upregulates fibroblast contractile activity. *Mol. Biol. Cell.* 12:2730–2741.
35. Hossain, M. M., J. F. Crish, R. L. Eckert, J. J. Lin, and J. P. Jin. 2005. h2-Calponin is regulated by mechanical tension and modifies the function of actin cytoskeleton. *J. Biol. Chem.* 280:42442–42453.
36. D'Addario, M., P. D. Arora, J. Fan, B. Ganss, R. P. Ellen, and C. A. McCulloch. 2001. Cytoprotection against mechanical forces delivered through beta 1 integrins requires induction of filamin A. *J. Biol. Chem.* 276:31969–31977.
37. Wang, N., and D. Stamenovic. 2000. Contribution of intermediate filaments to cell stiffness, stiffening, and growth. *Am. J. Physiol. Cell Physiol.* 279:C188–C194.
38. Wang, N., and D. Stamenovic. 2002. Mechanics of vimentin intermediate filaments. *J. Muscle Res. Cell Motil.* 23:535–540.
39. Chen, C. S., and D. E. Ingber. 1999. Tensegrity and mechanoregulation: from skeleton to cytoskeleton. *Osteoarthritis Cartilage.* 7: 81–94.
40. Rosenblatt, N., S. Hu, B. Suki, N. Wang, and D. Stamenovic. 2007. Contributions of the active and passive components of the cytoskeletal prestress to stiffening of airway smooth muscle cells. *Ann. Biomed. Eng.* 35:224–234.
41. Wang, N., I. M. Tolic-Norrelykke, J. Chen, S. M. Mijailovich, J. P. Butler, J. J. Fredberg, and D. Stamenovic. 2002. Cell prestress. I. Stiffness and prestress are closely associated in adherent contractile cells. *Am. J. Physiol. Cell Physiol.* 282:C606–C616.
42. Stamenovic, D. 2005. Effects of cytoskeletal prestress on cell rheological behavior. *Acta Biomater.* 1:255–262.
43. Janmey, P. A., M. E. McCormick, S. Rammensee, J. L. Leight, P. C. Georges, and F. C. MacKintosh. 2007. Negative normal stress in semiflexible biopolymer gels. *Nat. Mater.* 6:48–51.

44. Mizuno, D., C. Tardin, C. F. Schmidt, and F. C. Mackintosh. 2007. Nonequilibrium mechanics of active cytoskeletal networks. *Science*. 315:370–373.

45. Fernandez, P., P. A. Pullarkat, and A. Ott. 2006. A master relation defines the nonlinear viscoelasticity of single fibroblasts. *Biophys. J*. 90:3796–3805.

46. Bischofs, I. B., and U. S. Schwarz. 2003. Cell organization in soft media due to active mechanosensing. *Proc. Natl. Acad. Sci. USA*. 100:9274–9279.

47. Kong, H. J., T. R. Polte, E. Alsberg, and D. J. Mooney. 2005. FRET measurements of cell-traction forces and nano-scale clustering of adhesion ligands varied by substrate stiffness. *Proc. Natl. Acad. Sci. USA*. 102:4300–4305.

48. Saez, A., A. Buguin, P. Silberzan, and B. Ladoux. 2005. Is the mechanical activity of epithelial cells controlled by deformations or forces? *Biophys. J*. 89:L52–54.

49. Ladam, G., L. Vonna, and E. Sackmann. 2005. Protrusion force transmission of amoeboid cells crawling on soft biological tissue. *Acta Biomater*. 1:485–497.